OFFICE OF NAVAL RESEARCH

Contract N00014-94-1-0323

R&T Code 413v001

Technical Report No. 3

ELECTRIC FIELD-INDUCED TRANSITIONS OF AMPHIPHILIC LAYERS ON Hg ELECTRODES

by

Xiaoping Gao, Henry S. White, Shaowei Chen
and Hector D. Abruna

Submitted for publication

Langmuir

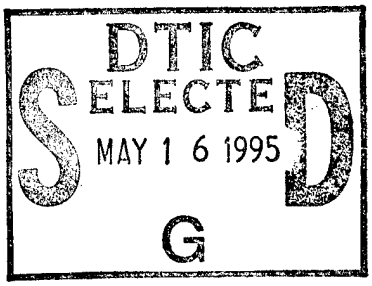

University of Utah
Department of Chemistry
Salt Lake City, UT 84112

April 31, 1995

REPORT DOCUMENTATION PAGE

Form Approved
OMB No. 0704-0188

1. AGENCY USE ONLY (Leave blank)	2. REPORT DATE	3. REPORT TYPE AND DATES COVERED
	3/31/95	Interim 6/94 - 12/94

4. TITLE AND SUBTITLE

Electric Field-Induced Transitions of Amphiphilic Layers on Hg Electrodes

5. FUNDING NUMBERS

N0014-94-1-0323

R & T Code 413V001

6. AUTHOR(S)

Xiaoping Gao, Henry S. White, Shaowei Chen and Hector D. Abruna

7. PERFORMING ORGANIZATION NAME(S) AND ADDRESS(ES)

Department of Chemistry
Henry Eyring Building
University of Utah
Salt Lake City, Utah 84112

8. PERFORMING ORGANIZATION REPORT NUMBER

3

9. SPONSORING / MONITORING AGENCY NAME(S) AND ADDRESS(ES)

Office of Naval Research
800 North Quincy Street
Arlington, Virginia

10. SPONSORING / MONITORING AGENCY REPORT NUMBER

Accesion For
NTIS CRA&I [X]
DTIC TAB [ ]
Unannounced [ ]
Justification

By
Distribution /

11. SUPPLEMENTARY NOTES

12a. DISTRIBUTION / AVAILABILITY STATEMENT

Unclassified/Unlimited

Availability Codes

Dist	Avail and / or Special
A-1	

12b. DISTRIBUTION CODE

13. ABSTRACT (Maximum 200 words)

There are numerous examples in the literature of amphiphilic molecules which, when adsorbed onto mercury electrodes, undergo electric field-induced transitions between different molecular conformations. In general, very sharp and reversible voltammetric features associated with these transitions are observed when the electrode potential is scanned in the negative direction, typically over the range of -0.30 to -1.50 V vs SCE, although no redox center is active in these molecular assemblies within this potential range. Using simple electrostatic and thermodynamic arguments, an analytical expression is derived that allows the voltammetric response to be computed in terms of possible molecular conformational changes of the monolayer. The magnitude, shape, and potential of the voltammetric wave are dependent upon molecular parameters (e.g., charge distribution, dimensions and dielectric properties of the amphiphile), surface coverage, and non-electrostatic energy contributions. A peak-shaped voltammetric response is shown to be consistent with the redistribution of charged sites within the amphiphilic layer in response to the surface electric field. Numerical results are in qualitative agreement with voltammetric data for dioleoylphosphatidylcholine (DOPC) adsorbed onto mercury electrodes.

14. SUBJECT TERMS

15. NUMBER OF PAGES

16. PRICE CODE

17. SECURITY CLASSIFICATION OF REPORT	18. SECURITY CLASSIFICATION OF THIS PAGE	19. SECURITY CLASSIFICATION OF ABSTRACT	20. LIMITATION OF ABSTRACT
Unclassified	Unclassified	Unclassified	

Standard Form 298 (Rev. 2-89)

Electric Field-Induced Transitions of Amphiphilic Layers on Hg Electrodes

Xiaoping Gao, Henry S. White*
Department of Chemistry, University of Utah, Salt Lake City, UT 84112

Shaowei Chen, and Héctor D. Abruña*
Department of Chemistry, Baker Laboratory, Cornell University, Ithaca, NY 14853

Abstract: There are numerous examples in the literature of amphiphilic molecules which, when adsorbed onto mercury electrodes, undergo electric field-induced transitions between different molecular conformations. In general, very sharp and reversible voltammetric features associated with these transitions are observed when the electrode potential is scanned in the negative direction, typically over the range of -0.30 to -1.50 V vs SCE, although no redox center is active in these molecular assemblies within this potential range. Using simple electrostatic and thermodynamic arguments, an analytical expression is derived that allows the voltammetric response to be computed in terms of possible molecular conformational changes of the monolayer. The magnitude, shape, and potential of the voltammetric wave are dependent upon molecular parameters (e.g., charge distribution, dimensions and dielectric properties of the amphiphile), surface coverage, and non-electrostatic energy contributions. A peak-shaped voltammetric response is shown to be consistent with the redistribution of charged sites within the amphiphilic layer in response to the surface electric field. Numerical results are in qualitative agreement with voltammetric data for dioleoylphosphatidylcholine (DOPC) adsorbed onto mercury electrodes.

Submitted to *Langmuir*, April, 1995

Introduction: Amphiphilic molecules, including phospholipid monolayers, have been employed as models for biological membranes in the study of membrane structural transitions and membrane transport [1-6]. Due to the mechanical stability of these layers and their strong resistance to oxidation or reduction, electrochemical techniques have proven quite valuable in the investigation of the electrical properties of these model membranes. Of particular note is the work of Miller and co-workers and Lecompte and coworkers [7-11]. These investigators studied, employing impedance measurements and cyclic voltammetry, the electrochemical behavior of a variety of molecules such as prothrombin at mercury electrodes coated with amphiphilic monolayers and in some cases directly onto the mercury surface itself. Their studies suggested that there was an electrode potential-induced reorientation of the amphiphilic molecules adsorbed onto mercury.

In more recent investigations, voltammetric techniques have been used to study potential-induced structural changes of phospholipid monolayers that are irreversibly adsorbed onto a Hg electrode [12-14]. For example, Figure 1 presents a steady-state cyclic voltammogram in a 0.20 M KCl solution (at a sweep rate of 100 V/sec) for a Hg electrode coated with an irreversibly-adsorbed monolayer of dioleoylphosphatidylcholine (DOPC, see structure below).

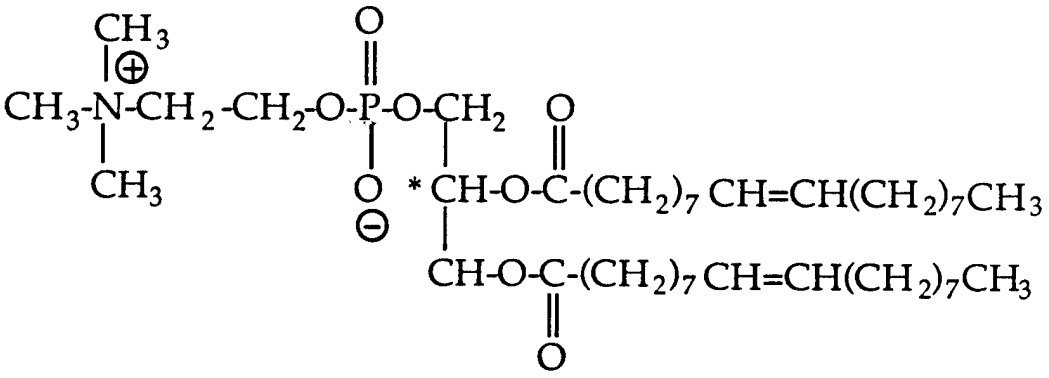

structure of DOPC

Although no redox active center (within the potential range of 0.0 to -1.5 V vs SSCE) is present in these molecular assemblies, two very sharp, and reversible waves are observed with peak potentials of -0.90 and -1.1 V, respectively.

The peak-shape voltammetric response shown in Fig. 1 is typical of Hg electrodes coated with electroinactive long-chain carboxylic acids [15], as well as other phospholipids [12,13]. The number of voltammetric waves observed and the electrode potential at which they occur are specific to the chemical nature of the monolayer. However, in all of these cases, the voltammetric response is unquestionably associated with a conformational change within the monolayer, since the molecules that comprise the monolayer are electroinactive within the investigated potential range. We find evidence for such behavior in a variety of publications where amphiphilic *redox-active* molecules adsorbed onto mercury surfaces exhibit additional voltammetric features that are not associated with the redox center in question. Recent examples of these include the work of Schiffrin [16] and co-workers on the electrochemical behavior ubiquinone (UQ_{10}) adsorbed onto mercury electrodes as well as the work of Tokuda and co-workers [17,18] and Camacho and co-workers [19] on long chain viologens. In all of these cases there is a voltammetric feature, not associated with the redox active center, which can be ascribed to the afore-mentioned potential-induced conformational transitions.

Although there is a qualitative understanding that a transient current will result whenever there is a potential-induced re-distribution of surface charge (the above response for adsorbed DOPC (Figure 1) clearly illustrates such behavior), to our knowledge, no theoretical treatment exists which describes the current-voltage response associated with such a process. In the specific case of phospholipid monolayers on Hg electrodes, there have been limited attempts at developing a theoretical framework that allows interpretation of the voltammetric response. Nelson and Leermakers used a statistical model based on Flory-Huggins (F-H) interaction parameters to elucidate the potential-dependent structures of phospholipid monolayers and bilayers on Hg in equilibrium with a solution containing

the phospholipid molecule [13]. Based on their computations, these authors suggested that the first voltammetric peak in Figure 1 "corresponds to a competition between head groups and hydrocarbon tails for access to the interface giving rise to an inhomogeneous layer of two phases consisting of a thin bilayer and thin monolayer respectively" [13b], consistent with the reorientation of some fraction of the molecules comprising the film from a tails-down to head-group-down conformation. This behavior is rationalized by assuming that the affinities of the solvent (H_2O), head group, and apolar hydrocarbon tails for the surface are strong functions of the surface hydrophobicity, which is electrode potential dependent and decreases as the electrode potential is moved away from the potential of zero charge (E_{pzc}). Although this description is quite reasonable, unfortunately, no structurally-sensitive experimental measurements (e.g., in-situ STM or x-ray diffraction methods) have been made that either support or refute the proposed potential-dependent structures. In addition, values of the F-H interaction parameters for the various potential-dependent surface interactions are not known [13a].

More recent theoretical and experimental investigations by Wängnerud and Jönsson have focused of the physical nature of interactions that give rise to adsorption of amphiphiles as bilayers on charged surfaces, including, among several factors, the influence of electrostatic interactions between the surface and charged adsorbed molecules [20]. In this work, electrostatic effects are explicitly treated using the Poisson-Boltzmann equation, yielding testable predictions concerning the nature of adsorbed structures as a function of the surface charge density, electrolyte concentration, and valence of the amphiphile co-ion. A key conclusion of the Wängnerud and Jönsson investigations, supported by in-situ ellipsometry, is that the structure of the amphiphile layer is strongly dependent on electrostatic effects, tending to form bilayers at high surface charge densities.

Following the general approach of Wängnerud and Jönsson, a peak-shaped current in the voltammetric response of amphiphilic monolayers irreversibly-adsorbed onto Hg can be anticipated by considering the electrostatic forces acting between the charged metal

surface and the ionized head groups on a lipid layer. Consider, for instance, the idealized structures shown in Figure 2 of a lipid monolayer in contact with a metal electrode and immersed in an electrolytic solution. For simplicity, we assume that the molecule has a positively-charged head group and that it is possible for the molecule to rapidly change between orientations in which the head group is at the metal/lipid interface or at the lipid/solution interface. When the potential of the electrode is sufficiently positive of the potential of zero charge ($E > E_{PZC}$), such that the electrode surface has a net positive charge density, there will be a tendency for the molecules to orient such that the head groups are located at the lipid/solution interface, thereby reducing the electrostatic repulsion between the surface and lipid layer. Conversely, when the electrode potential is negative of the E_{PZC}, the electrostatic attraction between the negatively charged electrode and positively charged molecule will tend to orient the molecule with the head group at the metal/lipid layer interface.

The reorientation of the lipid layer results in the movement of a net charge through the electric field that exists across the lipid layer. For the phospholipids corresponding to the data in Figure 1, the effective distance that charge is moved is on the order of the length of the molecule (~25Å). This displacement of charge will alter the preexisting electric field, resulting in a measurable flow of current at the electrode surface. This current is associated only with charging of the interface required to minimize the electrical energy (and, thus, overall free energy) and does not involve any redox chemistry.

Although the structures and conformational transition depicted in Figure 2 are highly speculative, and perhaps unrealistic based on energetic considerations, we will employ this model for the sole purpose of demonstrating a general method of computing the voltammetric current resulting from a potential-dependent conformational change. As will be discussed in a later section, the methodology described here may be readily adapted to other structures (including amphiphilic bilayers), as well as other potential-dependent

interactions (such as solvent dipole reorientation), allowing the voltammetric response to be computed for structures that are deduced from future experimental measurements.

As noted above, no theoretical treatment exists which allows prediction or interpretation of the voltammetric response associated with such a conformational transition. Consequently, prior voltammetric investigations of amphiphilic monolayers have not provided quantitative information concerning the structural features of the monolayer nor the dynamics of potential-dependent conformational changes. On the other hand, voltammetric techniques for investigating electroactive monolayers, e.g., self-assembled monolayers with pendant redox groups [21], are well-established and provide a quantitative means of measuring kinetic and thermodynamic parameters associated with electron-transfer, the number density of electroactive molecules within the film, and the chemical stability of the monolayer in different oxidation states [22]. In addition, recent theoretical and experimental investigations have shown that the voltammetric response of an irreversibly-adsorbed electroactive monolayer [23], and monolayers containing acid/base groups [24], are very sensitive to structural details of the adsorbed molecule (e.g., chain length, valence) as well as to parameters that influence the interfacial potential distribution (e.g., ionic strength of the contacting solution). These latter developments suggest that similar structural information concerning amphiphilic films might be obtained by electrochemical measurements.

Based on the success of voltammetric techniques in characterizing electroactive films, our laboratories have recently initiated an investigation of the factors that determine the peak-shaped voltammetric response of nonelectroactive monolayers, with the prospect of applying the results to amphiphilic monolayers. This report describes a first approach based on integrating electrostatic and thermodynamic arguments describing the film conformations, with the relevant equations describing the perturbation and response functions of the voltammetric experiment. Because of the mathematical complexities that underlie an accurate description of the film structure, especially at the microscopic level, as

well as those associated with the electroanalytical method, a number of simplifications have been made in order to yield a tractable problem. Nevertheless, the results represent the first quantitative model of the voltammetric response of an electroinactive amphiphilic monolayer, and are conceptually useful in understanding how the peak-shaped current response is related to the structure of the monolayer and its electrostatic environment.

Experimental. Dioleoylphosphatidylcholine (DOPC, approximately 99%) was used as received from Fluka. Solutions of 0.20 mg of DOPC per mL of chloroform were prepared just prior to use. Electrolyte solutions were prepared with ultrapure (at least 99.99+%) salts (Aldrich), which were dissolved (0.20 M) in water which was purified with a Milli-Q system and buffered with high purity phosphate salts or hydrochloric acid (all from Aldrich) depending on the desired pH.

Electrochemical experiments were carried out with an EG&G PARC 173 potentiastat and 175 Universal Programmer. Data were collected on a Nicolet 4094 digital oscilloscope and transferred to a personal computer for analysis.

A sodium-saturated calomel electrode (SSCE) was used as the reference electrode and a large area platinum coil was used as the counter electrode. The working electrode was a Kemula type (micrometer driven) hanging mercury drop electrode (HMDE), which was filled with high purity mercury (electronic grade, 99.9998% from Johnson Matthey). A two-compartment cell without frits was employed in all experiments. The cell had standard joints for all electrodes and for degassing.

The detailed experimental procedures have been described previously [12, 14]. Figure 1 shows the typical voltammetric response (at 100 V/sec) for a DOPC monolayer adsorbed on a Hg electrode surface in a 0.20 M KCl solution (pH=8.2). Two very sharp and reversible waves centered at about -0.9 and -1.0 V, respectively, are clearly evident. A qualitatively similar response was observed over the pH range from 0.7 to 9.2. However, the potentials at which these two waves appeared as well as their sharpness were dependent

on pH and on the nature of the electrolyte. Such effects and trends have been reported earlier [12].

Results and Discussion. An expression that describes the voltammetric behavior of electroinactive lipid layers is developed in the following order. In Section I, an electrostatic model of the interface that incorporates the essential features of the assembled phospholipid layer is introduced. General analytic expressions are presented which relate the applied electrode potential in a voltammetric experiment to the orientation of the lipid molecules on the surface and to other electrostatic parameters that influence the overall interfacial charge and potential distributions (e.g., electrolyte concentration and dielectric constant). In Section II, an expression for the free energy of the lipid molecules is introduced which allows the configuration of the molecular layer to be computed as a function of the interfacial potential distribution. The electrostatic and thermodynamic expressions are combined in Section III to obtain the general current-potential response expected in a voltammetric experiment. In Section IV, theoretical voltammograms are presented for a variety of system parameters (e.g., surface coverage, molecular dimensions, degree of lipid ionization), and, in Section V, the results are compared to experimental data.

The general strategy used in developing a model for the voltammetric response of these lipid monolayers is similar to that reported earlier for analyzing the behavior of the monolayers containing redox or acid/base functionalities [23,24].

I. *Interfacial Potential and Charge Distribution.* Figure 3 shows the electrostatic model used to compute the interfacial potential distribution. The model consists of a tightly-packed lipid monolayer assembled on a planar metal electrode of area A (cm^2) and immersed in an electrolyte solution that contains a symmetric z:z electrolyte. The solution is assigned a dielectric constant, ε_s.

The lipid monolayer assembly can be modeled in several ways that strongly depend on the assumed molecular conformation and the degree of dissociation of head group functionalities. For instance, at moderate and high pH, DOPC exists as a zwitterionic species (see structure); whereas at low pH (pH<2), the phosphate group is protonated, leaving the head group with a net positive charge. As mentioned earlier, the voltammetric response is slightly dependent on pH, but two reversible voltammetric peaks, similar to the response shown in Figure 1, are observed at all pHs.

The model we assume, and schematically shown in Figure 3, is that of an electrode surface covered by two dielectric films of thicknesses d_1 and d_2 with dielectric constants, ϵ_1 and ϵ_2, respectively. The distance d_1 is defined as the distance between the surface and the positive site when the lipid head group is located at the electrode/lipid interface. It is difficult to obtain a precise value for d_1 without detailed structural information concerning the orientation of the head group at the surface. However, based on the molecular structure shown earlier, it is likely that this distance has a value between 2 and 3 Å. The thickness of the dielectric layer d_2 is defined as the length of the molecule, minus the length d_1. A transition between the inwards (head groups down) and outwards (tails down) orientations will result in a displacement of the positive charge on the molecule by a distance of $d_2 - d_1$.

The surface coverage of lipid molecules oriented with their polar head groups at the electrode/lipid and lipid/solution interfaces are designated as Γ_1 and Γ_2, respectively. Since the molecules are irreversibly adsorbed, the total surface coverage, Γ_T, is defined as $\Gamma_T = \Gamma_1 + \Gamma_2$.

To simplify the resulting expressions, we will assume each lipid molecule possesses a single net positive charge, z_{mol}. For the low pH DOPC structure, we anticipate $z_{mol} \sim +1$. From electrostatic considerations, at high pH, the zwitterionic form of DOPC would be expected to behave equivalently to a positively charged species, with z_{mol} less than +1. This conclusion is based on the dipole nature of the zwitterion, in which the positively charged choline group undergoes a slightly larger spatial translation

than the negatively-charged phosphate group (~4 - 6 Å based on the molecular dimensions discussed above) during the assumed conformational transition. Thus, the image charge (voltammetric current), induced in the metal during the conformational transition of the zwitterion will be equivalent to that generated by the transition of a molecule containing a small positive charge. However, these general arguments could be somewhat compromised by the fact that ion association between the amphiphilic molecules and dissolved counter-ions may be significant, albeit unknown [25]. As detailed below, this latter limitation prevents an independent measurement of z_{mol} and Γ_T using voltammetric data. However, the charge surface density, $z_{mol}\Gamma_T$, involved in the conformational transition is directly measurable.

Assuming that there is no charge in the film except that associated with the charged head groups ($0 \leq z_{mol} \leq +1$), the potential will decay linearly from ϕ_m to ϕ_1 and from ϕ_1 to ϕ_2. In the solution phase ($x > d_1 + d_2$), the potential is assumed to be governed by the Gouy-Chapman model and decays to ϕ_s in the bulk solution:

$$\tanh(ze(\phi(x)-\phi_s)/2kT) = \tanh(ze(\phi_2-\phi_s)/2kT)\exp(-\kappa(x-(d_1+d_2)))$$

where $\phi(x)$ is the potential (V) in the solution at position x, κ is the inverse Debye length (m^{-1}) given by $\kappa = \left(z^2e^2 2n^o/\varepsilon_o\varepsilon_s kT\right)^{1/2}$, e is the charge of an electron (C), n^o is the number concentration of the ions in the electrolyte (cm^{-3}), ε_o is the permitivity of free space ($C^2\,N^{-1}\,cm^{-2}$) and k is Boltzmann's constant (JK^{-1}).

In addition to the above assumptions, we also assume that charges on the metal surface (at x = 0) and on the head groups (at d_1 and d_1+d_2) are delocalized (i.e., discreteness of charge is ignored). Inclusion of the finite size of ions in the description of the electrochemical behavior of redox and acid/base functionalized monolayers on electrodes has been recently discussed by Fawcett and coworkers [23b,24b]. As will be shown below, the potential distribution of the system we are considering is dominated by the capacitance of the dielectric region corresponding to the hydrocarbon tail (i.e., the

region defined by $d_2 - d_1$). Thus, the approximation of delocalized charges outside of this region (i.e., at the metal and solution interfaces) appears reasonable.

The electrostatic force exerted on the lipid molecules at any applied electrode potential can be obtained by considering the relationship between the potential distribution and the charge densities on the metal, at positions d_1 and $(d_1 + d_2)$, and in the electrolyte solution. Since the electrode surface area is generally of the order of cm^2, and the interfacial distances d_1, d_2, and κ^{-1} are of the order of nm, it is only necessary to consider the potential distribution normal to the surface. With attention drawn to Figure 3, the electric field ($E = -\frac{dV}{dx}$) within each region of the interface is given by eq.1:

$$
\begin{array}{lll}
E = & 0 \quad (\because \varepsilon_m = \infty) & x < 0 \\
& (\phi_m - \phi_1)/d_1 & 0 < x < d_1 \\
& (\phi_1 - \phi_2)/d_2 & d_1 < x < (d_1 + d_2) \\
& \dfrac{\kappa 2kT}{ze} \sinh\left[\dfrac{ze(\phi_2(x) - \phi_s)}{2kT}\right] & x > d_1 + d_2 \\
& 0 & x \to \infty
\end{array} \qquad (1)
$$

The electric fields and the charge densities associated with the metal, lipid layer, and solution are related through Gauss' law. The Gaussian boxes shown in Fig. 3 enclose the charges of interest. For the assumed planar geometry, the electric field passes only through the faces of the boxes, each of surface area S. Thus:

$$Q_i = \varepsilon_o \varepsilon_i \int_S \vec{E}_i d\vec{S}_i = \varepsilon_o \varepsilon_i E_i S \qquad (2)$$

Combining eq. 1 and 2 and applying the result to the four boxes shown in Figure 3, yields the following system of equations relating the charge densities ($\sigma_i = Q_i/S$) and interfacial potentials.

$$\sigma_m = \varepsilon_o \varepsilon_1 (\phi_m - \phi_1)/d_1 \qquad \text{box 1} \qquad (3a)$$

$$\sigma_m + \sigma_1 = \varepsilon_o \varepsilon_2 (\phi_1 - \phi_2)/d_2 \qquad \text{box 2} \qquad (3b)$$

$$\sigma_{dif} = -\varepsilon_o \varepsilon_s \kappa \left(\frac{2kT}{ze}\right) \sinh\left(\frac{ze(\phi_2 - \phi_s)}{2kT}\right) \qquad \text{box 3} \qquad (3c)$$

$$\sigma_m + \sigma_1 + \sigma_2 + \sigma_{dif} = 0 \qquad \text{box 4} \qquad (3d)$$

where the definitions of charge densities ($C \cdot cm^{-2}$) on the electrode surface (σ_m), at the planes of the lipid head groups (σ_1, σ_2), and in the solution (the diffuse layer) (σ_{dif}) are given by eq. 4

$$\sigma_i = \begin{cases} \sigma_m & x = 0 \\ \sigma_1 & x = d \\ \sigma_2 & x = d_1 + d_2 \\ \sigma_{dif} & d_1 + d_2 < x < \infty. \end{cases} \qquad (4)$$

As has been indicated earlier, the lipid layer is electrochemically inactive and irreversibly adsorbed over the potential range of interest. Thus, the total charge per unit area in the film is constant, i.e.,

$$\sigma_1 + \sigma_2 = z_{mol} F \Gamma_T. \qquad (5)$$

II. *Relationship Between Local Potential and Molecular Orientation.* In order to calculate the voltammetric response corresponding to the field-induced transition, it is necessary to establish a relationship between the two assumed molecular orientations and the electrode

potential. As previously noted, the molecular orientation is anticipated to be a function of the applied potential if the electrostatic forces between the charges on the metal surface and on the lipid molecule are sufficiently large to flip the molecules between the inwards and outwards-directed configurations, Figure 2. The fact that a reversible voltammetric response, Figure 1, is observed even at relatively high scan rates (e.g., 100 V/s) suggests that this process is facile on the timescale of the electrochemical experiment, and that the equilibrium structure is determined, to a significant extent, by the interfacial potential distribution.

To account for the influence of the electrostatic potential on the molecular orientation, we assume that the electrochemical potential of the lipid molecules is given by

$$\overline{\mu}_j = \mu_j^o + RT \ln a_j + z_{mol} F \phi_j \tag{6}$$

where F, R and T are Faraday's constant (C mol^{-1}), the molar gas constant (J mol^{-1} K^{-1}), and the absolute temperature (K), respectively. The subscript j refers to the two possible molecular orientations (inwards (j = 1) and outwards (j = 2)) of the molecules adsorbed on the electrode surface. The constants μ_1^o and μ_2^o indicate non-electrostatic energy terms corresponding to hydrophobic/hydrophilic interactions, dispersion and solvation forces, and steric effects associated with the amphiphilic layer in the inwards and outwards orientations, respectively. We treat these terms as being independent of the electrode potential, since the predominant potential-dependent interactions with the electrode surface are likely to involve electrostatic forces between the surface charge and the fixed charge on the head group. The reader is referred to the thorough discussion of Wängnerud and Jönsson [20] for a detailed physical description and estimation of the non-electrostatic work terms.

At equilibrium, $\overline{\mu}_1 = \overline{\mu}_2$. Approximating the activities a_1 and a_2 by their respective surface concentrations, Γ_1 and Γ_2, yields the relationship between the electrostatic potential distribution in the film and the orientation of the charged sites:

$$\phi_1 - \phi_2 = -\frac{\mu_1^o - \mu_2^o}{z_{mol}F} - \frac{RT}{z_{mol}F}\ln\frac{\Gamma_1}{\Gamma_2}. \tag{7}$$

Eq. (7) is simplified by defining $f = \Gamma_1 / \Gamma_T$, and the potential, $E^o = -(\mu_1^o - \mu_2^o) / z_{mol}F$, yielding

$$\phi_1 - \phi_2 = E^o - \frac{RT}{z_{mol}F}\ln\left(\frac{f}{1-f}\right). \tag{8}$$

It is clear that the potential E^o represents the difference in the standard-state chemical potentials of the assumed molecular conformations, and, in this sense, its use is similar to that employed in defining the standard redox potentials of electron-transfer reactions (where μ_1^o and μ_2^o represent the standard-state chemical potentials of the reduced and oxidized partners of the redox couple). As detailed in a later section, the peak position of the voltammetric wave corresponding to a conformational transition is primarily determined by the value of E^o (versus a yet specified reference potential). Experimental variables that affect the electrostatic potential distribution (i.e., dielectric constant, ion concentration) have a smaller, but significant effect, on the potential at which the structural transition is observed.

Admittedly, the model that we have assumed for the potential-dependent conformational transition may not be necessarily correct, and clearly does not include all of the features necessary to describe the actual amphiphilic layer. However, although it is beyond the scope of this preliminary treatment, both the electrostatic and thermodynamic treatments outlined above may be readily modified when considering different structures

and potential dependent interactions. For instance, the Gaussian box approach used above can be readily extended to include a true zwitterionic structure, requiring only the addition of an additional charged layer in the model schematic (Figure 3) and one additional application of Gauss's law (eq. (2)). In analogous fashion, the electrostatic model can be extended to bilayer structures, and ion-association, and finite ion size effects may be included, as was recently done by Fawcett for self-assembled redox and acid/base monolayers. Similarly, the thermodynamic expressions we assume are highly idealized in many respects. A key deficiency is the implicit assumption that the energetics of reorientation of any molecule within the film are independent of the state of orientation of the neighboring molecules, i.e., the probability of a molecule being in an up or down configuration is independent of the orientational state of the neighboring molecules. Lateral electrostatic interactions within the film will likely make the random approximation improbable. This problem can be treated by methods similar to those developed by Levine [26] for accounting for lateral dipole-dipole interactions within adsorbed solvent layers, or in a more heuristic fashion by employing an adjustable interaction parameter in eq. (6) (equivalent to employing a Frumkin-type isotherm).

III. *Voltammetric Response.*

If the electrode potential is scanned at a constant rate ν (V/s), the voltammetric response of an electrode coated with an electrochemically-inert film is due only to the capacitive charging current.

$$i = \nu A C_T \tag{9}$$

In eq. (9), C_T is the total capacitance $\left(Fcm^{-2}\right)$ of the interface, which can be evaluated using the formal definition: $C_T = \partial\sigma_m / \partial E = \partial\sigma_m / \partial\phi_m$. In deriving an expression for C_T, it is convenient to define the following interfacial capacitances:

$$C_1 = \varepsilon_o \varepsilon_1 / d_1 \tag{10a}$$

$$C_2 = \varepsilon_o \varepsilon_2 / d_2 \tag{10b}$$

$$C_{dif} = \varepsilon_o \varepsilon_s \kappa \cosh\left[ze(\phi_2 - \phi_S)/2kT\right]. \tag{10c}$$

C_1 and C_2 represent the potential-independent capacitances of the film and C_{dif} is the potential-dependent diffuse layer capacitance.

The total interfacial potential drop (ϕ_m - ϕ_s) is equal to the sum of the individual contributions across the interface:

$$\phi_m - \phi_s = (\phi_m - \phi_1) + (\phi_1 - \phi_2) + (\phi_2 - \phi_s) \tag{11}$$

Substituting eqs. 3 and 10 into eq. 11 yields:

$$\phi_m = C_1^{-1}\sigma_m + C_2^{-1}(\sigma_m + \sigma_1) + \phi_2 \tag{12}$$

Differentiating eq. 12 with respect to σ_m yields the potential-dependent interfacial capacitance of the system:

$$C_T^{-1} = C_1^{-1} + C_2^{-1}\left(1 + \frac{\partial \sigma_1}{\partial \sigma_m}\right) + \frac{\partial \phi_2}{\partial \sigma_m} \tag{13}$$

Expressing the quantity $\partial\phi_2 / \partial\sigma_m$ as $(\partial\phi_2 / \partial\sigma_{dif}) / (\partial\sigma_m / \partial\sigma_{dif})$, and noting that $\partial\sigma_m / \partial\sigma_{dif} = -1$ (from eqs. 3d and 5), and $(\partial\phi_2 / \partial\sigma_{dif}) = -C_{dif}^{-1}$ (from eqs. 3c and 10c) yields

$$C_T^{-1} = C_1^{-1} + C_2^{-1}\left(1 + \frac{\partial \sigma_1}{\partial \sigma_m}\right) + C_{dif}^{-1} \tag{14}$$

An explicit expression for $\partial\sigma_1/\partial\sigma_m$ in terms of f is derived from the definition of σ_m. Substituting eq. 8 into eq. 3b (along with the definition $\sigma_1 = z_{mol} f F \Gamma_T$) yields

$$\sigma_m = \frac{\varepsilon_0 \varepsilon_2}{d_2}\left[E^o + \frac{RT}{z_{mol}F}\ln\left(\frac{1-f}{f}\right)\right] - z_{mol} f F \Gamma_T \tag{15}$$

which is differentiated with respect to σ_1:

$$\frac{\partial\sigma_1}{\partial\sigma_m} = \frac{\partial\sigma_1 / \partial f}{\partial\sigma_m / \partial f} = -\left[\frac{\varepsilon_o\varepsilon_2}{d_2}\frac{RT}{z_{mol}^2 F^2 \Gamma_T}\frac{1}{f(1-f)} + 1\right]^{-1} \tag{16}$$

Since $0 \le f \le 1$, the bracketed expression of eq.16 is always positive, and therefore $\partial\sigma_1 / \partial\sigma_m$ must always be negative. Physically, this relationship indicates that an increase in the positive charge on the electrode must result in a decrease in the positive charge at x = d_1, and conversely, that an increase in the negative surface charge will result in an increase in the positive charge at d_1.

Combining eqs. 9, 14, and 16 yields the voltammetric current for the amphiphilic monolayer-coated electrode in terms of f.

$$i = \nu A\left\{C_1^{-1} + C_2^{-1}\left(1 - \left[\frac{\varepsilon_o\varepsilon_2}{d_2}\frac{RT}{z_{mol}^2 F^2 \Gamma_T}\frac{1}{f(1-f)} + 1\right]^{-1}\right) + C_{dif}^{-1}\right\}^{-1} \tag{17}$$

Before proceeding to the numerical calculations, it is instructive to note that the voltammetric current will be dominated by the smallest individual capacitance of the interface. Consider, for example, a lipid layer with $d_1 \approx 4$ Å, $d_2 = 30$ Å, and $\varepsilon_1 = \varepsilon_2 = 4$, immersed in an aqueous solution containing 0.10 M of a 1:1 supporting electrolyte ($\varepsilon_s = 78$ and $\kappa^{-1} \sim 10$ Å). From eq. 10, $C_1 \approx 10\mu F / cm^2$, $C_2 \approx 1.5\mu F / cm^2$ and $C_{dif}^{\min} \approx 90\mu F / cm^2$

(where C_{dif}^{min} is the minimum diffuse layer capacitance evaluated at $\phi_2 = \phi_S$). Thus, the voltammetric current will be dominated by the capacitance associated with the hydrocarbon tail, C_2, and the variation of $C_2^{-1}(1+\partial\sigma_1/\partial\sigma_m)$, eq. 14, with the electrode potential will largely determine the shape of the voltammetric response. A maximum in the voltammetric curve is expected, since as the film structure changes from a fully inwards orientation (f = 1) to a fully outwards orientation (f = 0), the quantity $(\partial\sigma_1/\partial\sigma_m)$ changes from 0 to a negative value (see eq. 16), and $C_2^{-1}(1+\partial\sigma_1/\partial\sigma_m)$ decreases.

As the film becomes either completely head group directed inward or outwards relative to the electrode surface (i.e., as $f \to 1$ or $f \to 0$), $\partial\sigma_1/\partial\sigma_m \to 0$ and eq. 14 reduces to the expression for the total capacitance of a film in which no conformational changes are present.

$$C_T^{-1} = C_1^{-1} + C_2^{-1} + C_{dif}^{-1} \tag{18}$$

IV. *Computational Results.*

The voltammetric response is obtained by calculating the current and applied potential as a function of f. The current, i, is obtained directly from eq. (17). An explicit expression for the electrode potential, E (= ϕ_m - ϕ_S), is readily obtained by solving eq. (3c) for ϕ_2 (using the identity $\sinh^{-1}[u] = \ln[u + (u^2 + 1)^{0.5}]$), and substituting the result into eq. 12, along with the definitions $\sigma_1 = z_{mol}f F\Gamma_T$, $\sigma_1 + \sigma_2 = z_{mol}F\Gamma_T$, and $\sigma_{dif} = -(\sigma_m + \sigma_1 + \sigma_2)$ (eq. 3d). The result is given in eq. (19), where σ_m (eq. (15)) is computed for each specified value of f.

$$E = C_1^{-1}\sigma_m + C_2^{-1}(\sigma_m + z_{mol}fF\Gamma_T) + (2kT/ze)\ln\left\{\frac{ze(\sigma_m + z_{mol}F\Gamma_T)}{2\varepsilon_o\varepsilon_s\kappa kT} + \left[1 + \left(\frac{ze(\sigma_m + z_{mol}F\Gamma_T)}{2\varepsilon_o\varepsilon_s\kappa kT}\right)^2\right]^{0.5}\right\} \tag{19}$$

Eqs. (17) and (19) completely describe the voltammetric response in terms of the properties of the lipid layer (surface coverage, charge, molecular dimensions and dielectric), the solution phase (electrolyte concentration, charge, and solution dielectric), and temperature. The following independent parameters are input into each calculation: E^o, $\varepsilon_o\varepsilon_1/d_1$ (= C_1), $\varepsilon_o\varepsilon_2/d_2$ (= C_2), $z_{mol}\Gamma_T$, κ^{-1}, z, T, ν, and A. All calculations presented are computed for T = 300 K and z = 1. Unless stated otherwise, E^o is taken equal to E_{PZC} (i.e., $E^o = 0$). Anodic and cathodic currents are mirror images of each other, since the lipid layer is assumed to be in equilibrium with the electrode potential at all times. Only the cathodic current will be presented in the figures. Electrode potentials, E, are referenced to the potential of zero charge, E_{pzc}, of the bare electrode (i.e., in the absence of the adsorbate; as shown below, the adsorption of the lipid layer induces a significant shift in the E_{pzc}). Voltammetric currents are normalized to the scan rate and electrode area ($i/\nu A$).

Figure 4 shows a voltammogram calculated using the following parameters: z_{mol} = 0.5, Γ_T = 6 x 10^{-11} mol/cm^2, ε_1/d_1 = 10/2, ε_2/d_2 = 6/33, ε_s = 78, and κ^{-1} = 9.6 Å (corresponding to a 0.10 M aqueous solution of a 1:1 electrolyte). These values are chosen to illustrate the general electrochemical behavior of a lipid monolayer-coated Hg electrode. In later sections, the effects of varying each parameter will be examined in detail.

Qualitatively, the shape of the theoretical voltammogram is in good agreement with the 1st voltammetric wave observed for a Hg/DOPC electrode in a pH 8.2, 0.20 M KCl solution (Figure 1). (As previously noted, the simplified model we have assumed does not account for the formation of the final bilayer structure, proposed as the origin of the 2nd cathodic wave [13]; thus, hereafter, all comparisons between experiment and theory refer only to the 1st wave.) A peak-shaped voltammetric response is observed, centered slightly negative of E_{PZC}. As shown below, the potential corresponding to the current maximum and the waveshape are dependent on E^o, z_{mol}, Γ_T, ε_s, κ^{-1}, and the capacitances of the lipid monolayer (ε_1/d_1 and ε_2/d_2).

The shape of the voltammetric wave, Figure 4, is similar to that expected for an electrode coated with an irreversibly adsorbed monolayer of an *electroactive* species. It is thus especially interesting that the theoretical voltammogram is entirely due to capacitive charging of the interface, and does not involve the transfer of electrons. A physical explanation of voltammetric response is illustrated in Figure 4, which shows the fraction of molecules with polar head groups oriented towards the interface, $f = \Gamma_1/\Gamma_T$ (dashed line), plotted as a function of the electrode potential. At positive potentials, i.e., $E > E_{PZC}$, f is essentially equal to 0, indicating that all of the lipid molecules in the film are oriented with their head groups oriented away from the interface. Under these conditions, the capacitance of the electrode is essentially constant, since the total electrode capacitance, $C_T^{-1} = C_1^{-1} + C_2^{-1} + C_{dif}^{-1}$, eq.(18), is dominated by the smallest individual capacitance, which corresponds to the potential-independent C_2. Consequently, a constant "background or baseline" charging current is observed at values of E sufficiently positive of E_{PZC}. The capacitance calculated from this constant current is ~2 $\mu F/cm^2$, in reasonable agreement with the experimental value obtained from Figure 1 (2.5 $\mu F/cm^2$). At potentials slightly positive of E_{PZC}, the lipid molecules that comprise the film begin to flip from an outwards orientation to an inwards orientation, due to the decrease in the electrostatic repulsion between the positive head groups and the positively charged surface. The quantity f increases monotonically as the potential is scanned negative of E_{PZC}, and at sufficiently negative potentials, f approaches 1 as the electrostatic attraction between the head groups and negative surface causes a complete inward-directed orientation of the molecular film.

Further insight into the origin of the voltammetric current is obtained by examining the charge density on the electrode surface, σ_m, as a function of the applied potential, E. Fig. 5 shows σ_m vs E (computed using eqs. (15) and (19)) for the same set of parameters used in computing the voltammetric response in Fig. 4. At potentials sufficiently positive or negative of the E_{PZC} the slope of σ_m vs. E is constant, indicating, as before, that the electrode capacitance ($C_T = \partial\sigma_m/\partial E$) is dominated by the potential-independent lipid-layer

capacitance, C_2. Near E_{pzc}, σ_m changes rapidly in response to the reorientation of adsorbed molecules. The peak-shaped voltammogram of Figure 4 is the result of the flow of electrons to the electrode surface (but not across the interface) in response to the field-induced movement of the positive charge on the lipid molecule towards the surface.

In general, the adsorption of a charged species from solution will induce a charge on the metal surface, the magnitude of which will depend on all parameters that affect the electrostatic potential distribution. For the adsorption of a positively charged phospholipid monolayer, the E_{PZC} shifts to a more positive potential. The plot of σ_m vs E, Figure 5, allows a graphical means of determining the shift in E_{PZC} due to adsorption of the lipid layer. The intersection of a horizontal dashed line corresponding to $\sigma_m = 0$ with the σ_m vs E curve defines the E_{PZC} after adsorption, which we will hereafter refer to as E_{PZC}^{ads}. This intersection occurs at 0.167 V vs E_{PZC}. Thus, adsorption of the charged lipid molecules onto the Hg surface results in a 0.167 V shift in the potential of zero charge [27].

Figure 6 shows the potential distribution across the lipid-coated electrode interface for values of f between 0.00034 and 0.99966, calculated using the same set of system parameters employed above. As anticipated from the previous results, most of the potential drop occurs across the region defined by the long hydrocarbon tail of the phospholipid (from d_1 to d_2). Regardless of the applied potential, the potential drop in the solution phase is small for electrolyte concentrations > 0.1 M, a consequence of $C_2 < C_{dif}$ for all values of f. Figure 6 also demonstrates that the E_{PZC} changes upon adsorption of a positively charge molecule. At E = 0 (which corresponds to E = E_{PZC} of the bare electrode) the electric field at the surface is seen to have a finite negative value, as evidence by the non-zero positive slope of the potential profile between x = 0 and x = d_1. Thus, it is immediately apparent that a finite negative charge exists on the electrode surface at this potential. The corresponding shift in the E_{PZC} to E_{PZC}^{ads} that results from this induced charge may be calculated as described in the previous paragraph.

Figures 7, 8, and 9 show the effects of varying the following parameters: E^o, Γ_T, C_{elec}, ε_1/d_1, ε_2/d_2. Varying E^o to be between $\pm$ 0.4 V has the effect of shifting the voltammetric wave on the potential axis, Figure 7, by an amount approximately equal to E^o. The linear dependence of the wave position on E^o is a consequence of the fact that virtually all of the interfacial potential drop occurs in the region between d_1 and d_2, as shown in Fig. 6 (i.e., $(\phi_1 - \phi_2) \approx E$, neglecting the small potential drops between $x = 0$ and d_1, and in the solution phase). The potential drop, $\phi_1 - \phi_2$, determines the conformation of the monolayer, and eq. (8) shows that changing the value of E^o has the effect of adding a constant value ($=E^o$) to the driving force that is necessary to induce the conformational transition. The key point here is that an experimental measurement of wave position (vs E_{PZC}) allows a direct estimation of the free energy change associated with the conformational transition. It is noteworthy that the voltammetric peak position is not determined by the sign of the charge associated with the polar head group. Thus, amphiphilic layers containing either negatively or positively charged head groups may exhibit transitions at potentials negative of E_{PZC}. The primary factor determining the peak potential, E_p, is the difference in the non-electrostatic energy contributions ($\mu_1^o - \mu_2^o$) of the two molecular conformations. In addition to the shift in E_p, the shape of the voltammetric wave has a finite, but very weak dependence on the value of E^o (the difference in the shapes of the three waves in Figure 8 is of the order of the width or the pen used to draw the curves).

An increase in Γ_T results in a proportional increase in the voltammetric peak height, Figure 8a (measured relative to the flat baseline capacitive current), in agreement with the predicted dependence of i on Γ_T indicated by eq. (17). Increasing the charge on the lipid molecule, z_{mol}, has a similar effect on the voltammetric response (not shown) as increasing Γ_T. In addition to increasing the peak height, an increase in z_{mol} also tends to cause a small broadening of the wave. However, since the dependencies of the voltammetric

response on z_{mol} and Γ_T are so similar, there is no simple means of separating the effects of these two factors.

The effect of varying the supporting electrolyte concentration, C_{elec}, on the voltammetric wave is shown Figure 8b. Lowering C_{elec} induces a significant positive shift in the voltammetric wave, indicating that the driving force for the conformational transition is slightly larger at more positive potentials. This behavior can be rationalized by noting that a decrease in C_{elec} causes a larger fraction of the total interfacial potential drop to occur across the diffuse double layer. From eq. 11, an increase in the diffuse double layer potential ($\phi_2 - \phi_s$), for any fixed electrode potential ($E = (\phi_m - \phi_s)$) results in a decrease in ($\phi_1 - \phi_2$), thereby increasing the driving force for the lipid molecules to reorient with their head groups towards the electrode surface (see eq. (7) and Figure 6). Thus, there is a positive shift in the position of the voltammetric wave.

As shown in Figure 9, the voltammetric response is a relatively strong function of the molecular parameters, ε_1/d_1 and ε_2/d_2. For example, decreasing ε_1/d_1 results in a dramatic decrease in the peak height, a broadening of the wave, and a shift in E_p to negative potentials. The dependence is analogous to that observed upon lowering C_{elec}, and is a consequence of the capacitance, C_1, (and, therefore the potential drop, $\phi_m - \phi_1$) in the region between $x = 0$ and d_1 becoming significantly larger as ε_2/d_2 decreases. Figure 9b shows that the primary effect of decreasing ε_2/d_2 is to increase the baseline capacitive current (that is, the effects in the figure are real) defined by eq. (18). For sufficiently large values of ε_2/d_2, the voltammetric wave becomes noticeably broadened, a result of C_2 becoming comparable to C_1 and C_{dif}.

For redox-active monolayers, the coverage (Γ_T (mol/cm^2) of electroactive molecules can be readily obtained from integration of the charge defined by the voltammetric wave [22]. No similar method of analysis exists in the literature for electrochemically-inert monolayers. To investigate the possibility of employing the voltammetric response in determining the surface coverage of DOPC on Hg, we have

numerically evaluated the charge under the theoretical voltammetric waves, Q_{app}, as a function of the charge corresponding to the actual coverage employed in the calculation, Q_f ($= z_{mol}F\Gamma_T$) [28]. The results are shown in Table I, as a function of the assumed values of the molecular parameters, ε_1/d_1 and ε_2/d_2 (other parameters used in the calculation are the same as in Fig.4). As seen in Table I, the charge measured underneath the voltammetric wave is always smaller than the actual value corresponding to the true surface coverage. However, the numerical examples presented in Table I show that Q_{app} is never more than ~25% smaller than Q_f over a wide range of ε_1/d_1 and ε_2/d_2 combinations. Thus, it is possible to obtain reasonably good estimates of Γ_T from the voltammetric response.

V. *Comparison of Experimental and Theoretical Voltammetric Response of Hg/DOPC.*

In Figure 10, data from Figure 1 are quantitatively compared to a theoretical voltammogram. Parameters used in computing the theoretical voltammogram were obtained as follows. A value of $\varepsilon_2/d_2 = 0.241$ Å^{-1} was computed from the potential-independent capacitive "baseline" current between -0.3 and -0.7 V, using the relationship $i/\nu A = C_T$ and the approximation $C_T \sim C_2$ (as discussed in the preceding section). Next, the peak potential of the experimental voltammogram, $E_p = -0.93$ V, referenced to the E_{PZC} of Hg in a non-adsorbing electrolyte ($E_{PZC} = -0.45$ V vs. SSCE in NaF), was used to compute a value of E^o for the lipid monolayer from the relationship $E^o \approx E_p - E_{PZC}$. The charge on the molecule was taken as +1, and the parameters T, C_{elec}, and z were given their respective experimental values. Finally, the parameters ε_1/d_1 and Γ_T were adjusted to yield the best visual fit of the theoretical curves to the data. Values of $\varepsilon_1/d_1 = 20$ Å^{-1} and $\Gamma_T = 2.2 \times 10^{-11}$ mol/cm^2 were obtained by this procedure.

The reasonable agreement between the theoretical and experimental voltammograms shown in Figure 10 supports the notion that the peak-shaped voltammogram results from a conformational transition within the lipid monolayer. However, as discussed above, our assumed structures are overly simplified, and do not include the possibility of bilayer

formation as proposed by Nelson and Leermakers [13]. The fitted value of $\varepsilon_2/d_2 = 0.241$ $Å^{-1}$, corresponds roughly to that expected based on a length of ~16 Å [29] and an effective dielectric constant of ~3.9. This value of ε_2 is in resonable agreement with that expected for the hydrocarbon tail region. On the other hand, the shape of the wave is not particularly sensitive to the chosen value of ε_1/d_1, for values of $\varepsilon_1/d_1 > 1$, as evident in Figure 9. Thus, our fitted value of $\varepsilon_1/d_1 = 20$ $Å^{-1}$ should not be interpreted as a precise value for this parameter. However, using a reasonable value of d_1 (~2 Å), gives a numerical value of ε_1=40, in good agreement with literature values [30].

The value of $\Gamma_T = 2.2 \times 10^{-11}$ mol/cm^2 obtained from the fitted data is approximately an order of magnitude smaller than that expected based on molecular models. Our underestimation of Γ_T may indicate that the charge per lipid molecule is considerably less than the assumed value of unity used in the calculation, or that only a fraction of the molecules undergo a conformational transition that results in the displacement of charge within the interfacial field. As noted previously, the height (and, thus, the area) of the voltammetric wave has essentially the same dependence on z_{mol} as Γ_T. Thus, a diminution of z_{mol} to 0.1 in the theoretical curve is equivalent to increasing Γ_T by a factor of 10.

The inset in Figure 10 shows the interfacial potential distribution corresponding to the calculated voltammogram. The curves show that the transition between the outwards and inwards directed conformation does not occur until the potential is significantly negative of the E_{PZC}, a consequence of the relatively greater stability of the monolayer conformation in which the charged head groups are oriented towards the polar solution phase.

Conclusions. A general analytical method has been developed that allows calculation of the voltammetric response of electrochemically-inert monolayers that are susceptible to field-induced conformational transitions. The model predicts the presence of peak shaped

voltammetric features which are quite consistent with numerous experimental observations. The method provides a means to determine the charge displacement and energetics associated with the conformational transition, and can easily be adapted to amphiphilic monolayers with structures and potential-dependent interactions different from those employed in this initial work. However, a rigorous test of this method will require input of potential-dependent structures obtained from direct experimental observations. We are currently carrying out in-situ X-ray reflectivity as well as in-plane surface X-ray diffraction studies of these systems which will allow us to make such quantitative comparisons in the future.

Acknowledgments. The authors gratefully acknowledge support from the Office of Naval Research (X.G., H.S.W., S.C. and H.D.A.) and National Science Foundation (grant DMR-9107116) (S.C. and H.D.A.).

References.

1. Blank, M.; Miller, I.R. *J. Colloid Interface Sci.* **1967**, 26, 26.
2. Phillips, M.C.; Chapman, D. *Biochim. Biophys. Acta* **1968**, 163, 301.
3. Sakurai, I.; Kawamura, Y. *Biochim. Biophys. Acta* . **1987**, 904, 405-409.
4. Seimiya, T.; Miyasaka, H.; Kato, T.; Shirakawa, T.; Ohbu, K.; Iwahashi, M. *Chem. Phys. Lipids* **1987**, 43, 161-177.
5. Ibdah, J.A.; Phillips, M.C. *Biochem.* **1988**, 27, 7155-7162.
6. Als-Nielsen, J.; Christensen, F.; Pershan, P.S. *Phys. Rev. Lett.* **1982**, 48, 1107.
7. Pagano, R. E.; Miller, I. R.; *J. Colloid Interface Sci.* **1973**, 45, 126
8. Lecompte, M. F.; Miller, I. R.; *Bioelectrochem. Bioeng*. **1988**, 20, 99
9. Lecompte, M. F.; Miller, I. R.; *J. Colloid Interface Sci.* **1988**, 123, 259
10. Lecompte, M. F.; Clavillier, J.; Dode, C.; Elion, J.; Miller, I. R.; *Bioelectrochem. Bioeng*. **1984**, 13, 211
11. Lecompte, M. F.; Miller, I. R.; *Biochemistry* **1980**, 19, 3439
12. Nelson, A.; Benton, A.*J. Electroanal. Chem.* **1986**, 202, 253-270.
13. (a) Leermakers, F.A.M.; Nelson, A. *J. Electroanal. Chem.* **1990**, 278, 53-72. (b) Nelson, A.; Leermakers, F.A.M. *J. Electroanal. Chem.* **1990**, 278, 73-83.
14. Chen, S. and Abruña, H.D. *Langmuir* **1994**, 10, 3343-3349.
15. Orzechowska, M. and Matysik, J. *J. Electroanal. Chem.* **1979**, 103, 251-259.
16. Gordillo, G. J.; Schiffrin, D. J. *J. Chem. Soc. Faraday Trans.* **1994**, 90, 1913
17. Kitamura, F.; Ohsaka, T.; Tokuuda, K. *J. Electroanal. Chem.* **1994**, 368, 281
18. Kitamura, F.; Ohsaka, T.; Tokuuda, K. *Chem Lett.* **1991**, 375
19. Sánchez Maestre, M.; Rodríguez-Amaro, R.; Muñoz, E.; Ruiz, J. J.; Camacho, L. *J. Electroanal. Chem.* **1993**, 359, 325
20. Wängnerud, B; Jönsson, B *Langmuir* **1994**, 10, 3268-78.
21. a. Chidsey, C.E.D. *Science* **1991**, 7, 919.
    b. Findklea, H. O.; Hanshew, D.D., *J. Am. Chem. Soc.* **1992**, 64, 2398.

c. Rowe, G. R.; Creager, S. E. *Langmuir* **1991**, 7, 2307.

22. Bard, A. J.; L. R. Faulkner *Electroanalytical Methods; J. Wiley*: New York, 1980.

23. a.Smith, C.P.; White, H.S. *Anal. Chem.* **1992**, 64, 2398-2405;

b. Fawcett, W. R. *J. Electroanal. Chem.* **1994**, 378, 117-24.

24. a. Smith, C. P.; White, H.S. *Langmuir* **1993**, 9, 1-3.

b. Fawcett, W. R., Fedurco, M.; Kovacova, *Langmuir* **1994**, 10, 2403-10.

25. Meijer, L.A.; Leermakers, F.A.M.; Nelson, A. *Langmuir* **1994**, 10, 1199-1206.

26. Levine, S.; Bell, G. M.; Smithe, A. L. *J. Phys. Chem.*, **1969**, 73, 3534.

27. A more precise value can be derived from eq. 12 by setting $\sigma_m = 0$ to yield $\phi_m^{pzc} = C_2^{-1}\sigma_1 + \phi_2$ where σ_1 is obtained from eq. 15, and ϕ_2 is calculated from eq. 3c and 3d, under the condition that $\sigma_m = 0$.

28. The following equation was employed to calculate Q_{app}:

$Q_{app} = [\sigma_m (f_0) - \sigma_m (f_1)] - C_T(f_0)[\phi_m(f_0) - \phi_m(f_1)]$

where $f_0 = 0.00001$ and $f_1 = 0.99999$, σ_m, C_T and ϕ_m are obtained from eq. 9, 14, and 13 respectively. First term is the total charge on the electrode surface and second term is the charge of the surface assuming there is no electroactive film. The capacitance for the second term is assumed as a constant, which is reasonable since the capacitance is dominated by C_2.

29. Wiener, M.C.; White, S. H. *Biophys. J.* **1992**, 61, 434-447.

30. Seelig, J.; Macdonald, P.M.; Scherer, P.G. *Biochem.* **1987**, 26, 7535-7541.

Table I. Comparison of Apparent (Q_{app}) and True (Q_f) Surface Coverage as a Function of Lipid Monolayer Parameters.

	Q_{app} (mC/m^2)[b]		
Q_f (mC/m^2)[a]	ε_1/d_1 = 2.5 $Å^{-1}$ ε_2/d_2 = 0.14	ε_1/d_1 = 0.5 $Å^{-1}$ ε_2/d_2 = 0.14	ε_1/d_1 = 2.5 $Å^{-1}$ ε_2/d_2 = 0.5
12	11	9	7
17	16	13	13
23	21	18	17
29	27	22	22
35	32	27	27
40	38	31	32
46	43	35	36
52	49	40	41
58	54	44	46
64	59	49	50

a) Q_f = charge corresponding to the true coverage ($z_{mol}F\Gamma_T$)

b) Q_{app} = charge determined from the integrated area under the calculated voltammetric wave (see text and ref. [27]).

Figure Captions.

1. Cyclic voltammetric responses of a Hg/DOPC electrode immersed in a N_2-purged 0.20 M KCl solution (pH = 8.2). Scan rate: 100 V/s.

2. Schematic diagram of the orientation of amphiphilic molecules in response to the electrode potential (relative to the potential of zero charge, E_{PZC}).

3. Model system used to calculate the charge distribution and electric field in the amphiphilic monolayer.

4. Voltammetric response (solid line) of Hg electrode coated with a amphiphilic monolayer, calculated from eqs. (17) and (19) using the following parameters: $E^o = 0$, $z_{mol} = 0.5$, $\Gamma_T = 6 \times 10^{-11}$ mol/cm^2, $\varepsilon_1/d_1 = 5$ Å^{-1}, $\varepsilon_2/d_2 = 0.182$ Å^{-1}, $C_{elec} = 0.10$ M, $z = 1$, $\varepsilon_3 = 78$, and T = 300 K. Fraction of lipid molecules ($f = \Gamma_1/\Gamma_T$) oriented with charged head group towards the electrode surface (dashed line).

5. Relationship between charge density on metal (σ_m) and electrode potential (E) The dashed line indicates the shift in the E_{PZC} due to the adsorbed monolayer (relative to a bare electrode). System parameters used in calculation are the same as in Fig. 4.

6. Potential distribution across the Hg/lipid monolayer interface as a function of applied potential, corresponding to the voltammetric response shown in Fig. 4.

7. Voltammetric response as a function of E^o. All other system parameters are the same as in Fig. 4.

8. Voltammetric response as a function of (a) surface coverage, Γ_T and (b) electrolyte concentration, C_{elec}. All other system parameters are the same as in Fig. 4.

9. Voltammetric response as a function of (a) ε_1/d_1 and (b) ε_2/d_2. All other system parameters are the same as in Fig. 4.

10. Comparison of experimental voltammogram (solid circles, data from Fig. 1) and theoretical response calculated using: $E^o = -0.475$ V, $E_{PZC} = -0.450$ vs SCE, $\Gamma_T = 2.2 \times 10^{-11}$ mol/cm^2, $z_{mol} = 1$, $C_{elec} = 0.10$ M, $\varepsilon_3 = 78$, $\varepsilon_1/d_1 = 20$ Å^{-1} and (b)

$\varepsilon_2/d_2 = 0.241$ Å^{-1}. The inset shows the interfacial potential distribution corresponding to the voltammetric response.

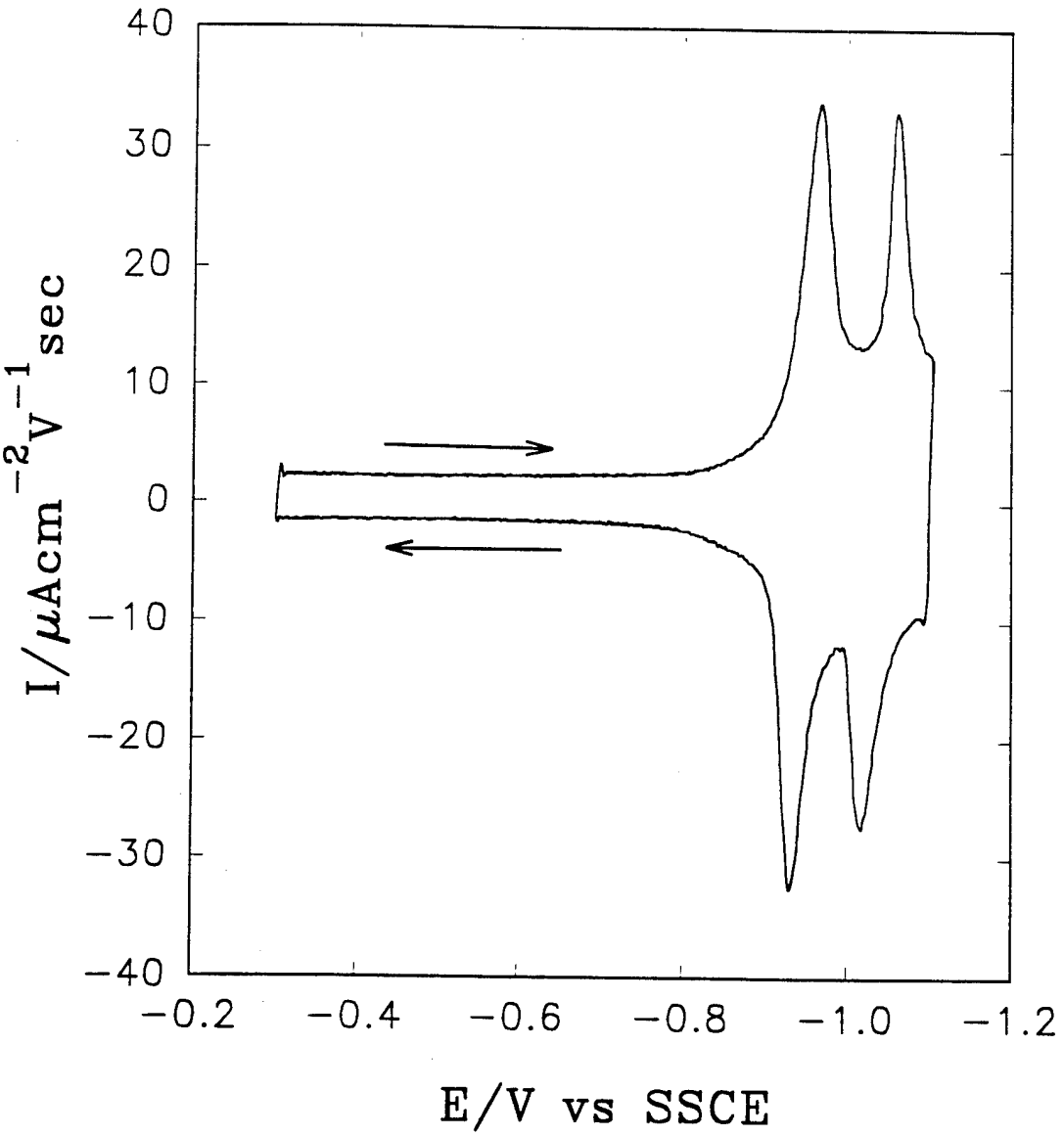

Figure 1

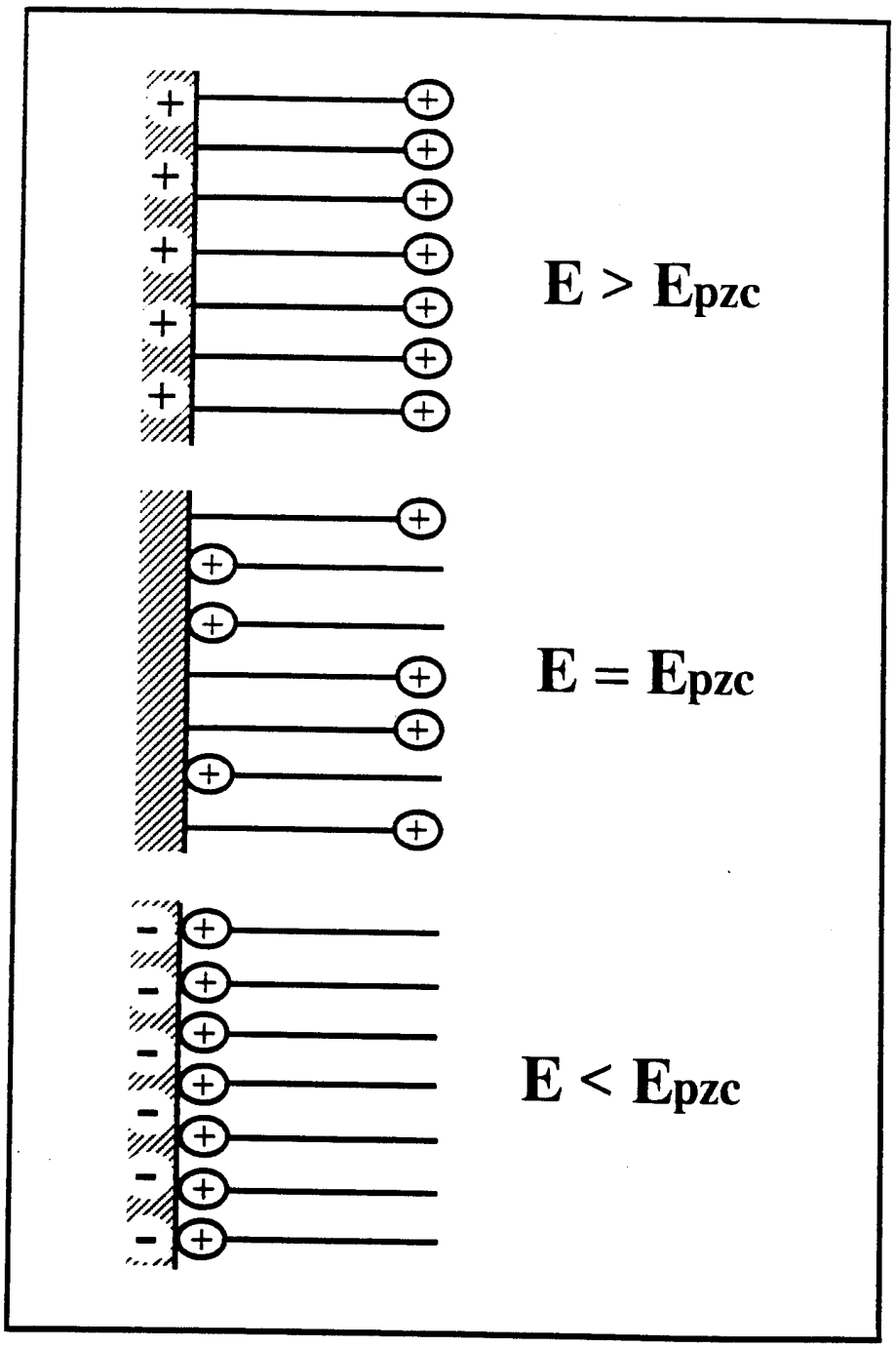

Fig. 2.

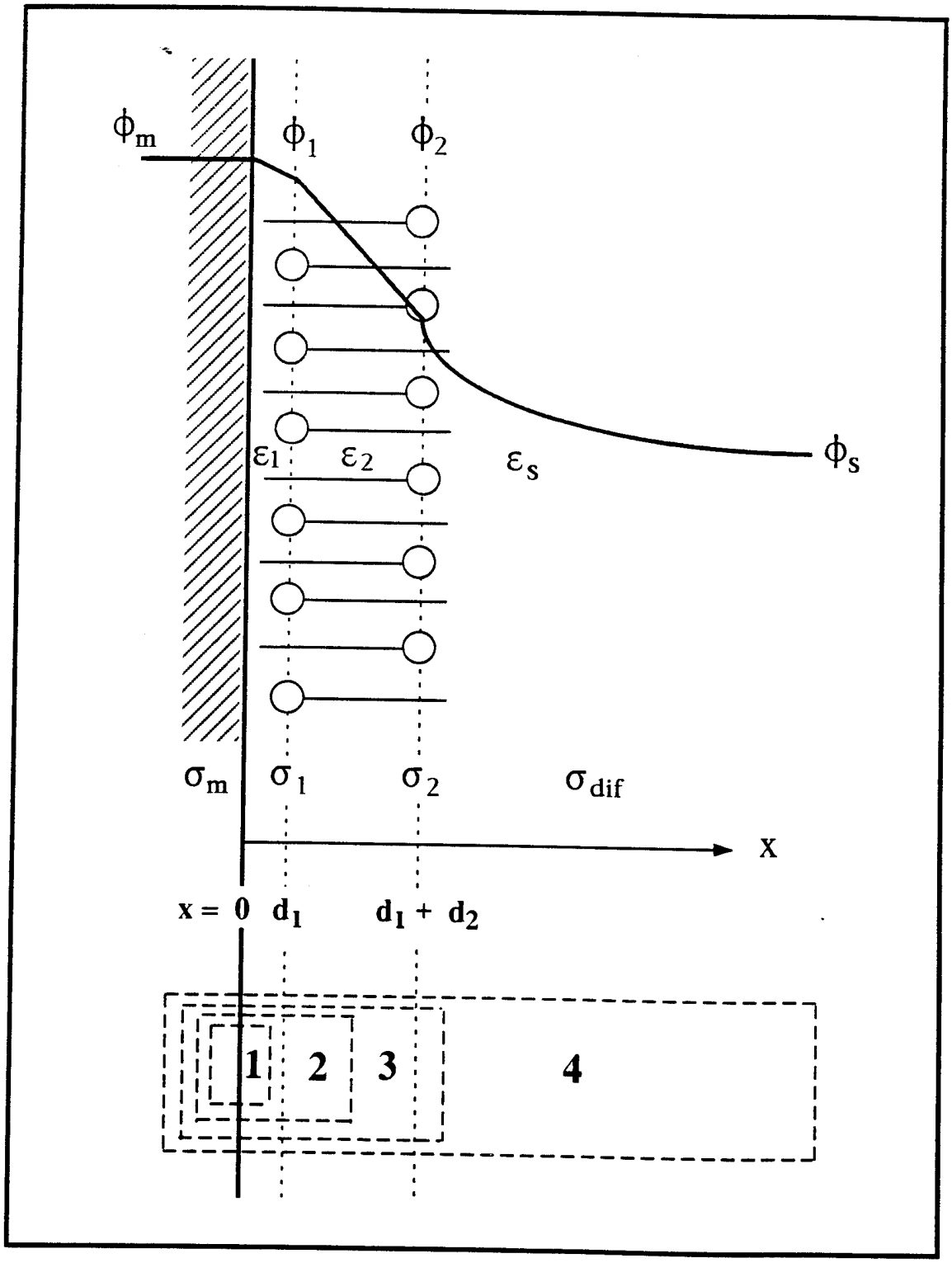
ϕ_m
ϕ_1
ϕ_2
ε_1
ε_2
ε_s
ϕ_s
σ_m
σ_1
σ_2
σ_{dif}
x
x = 0
d_1
$d_1 + d_2$
1
2
3
4

Fig 3

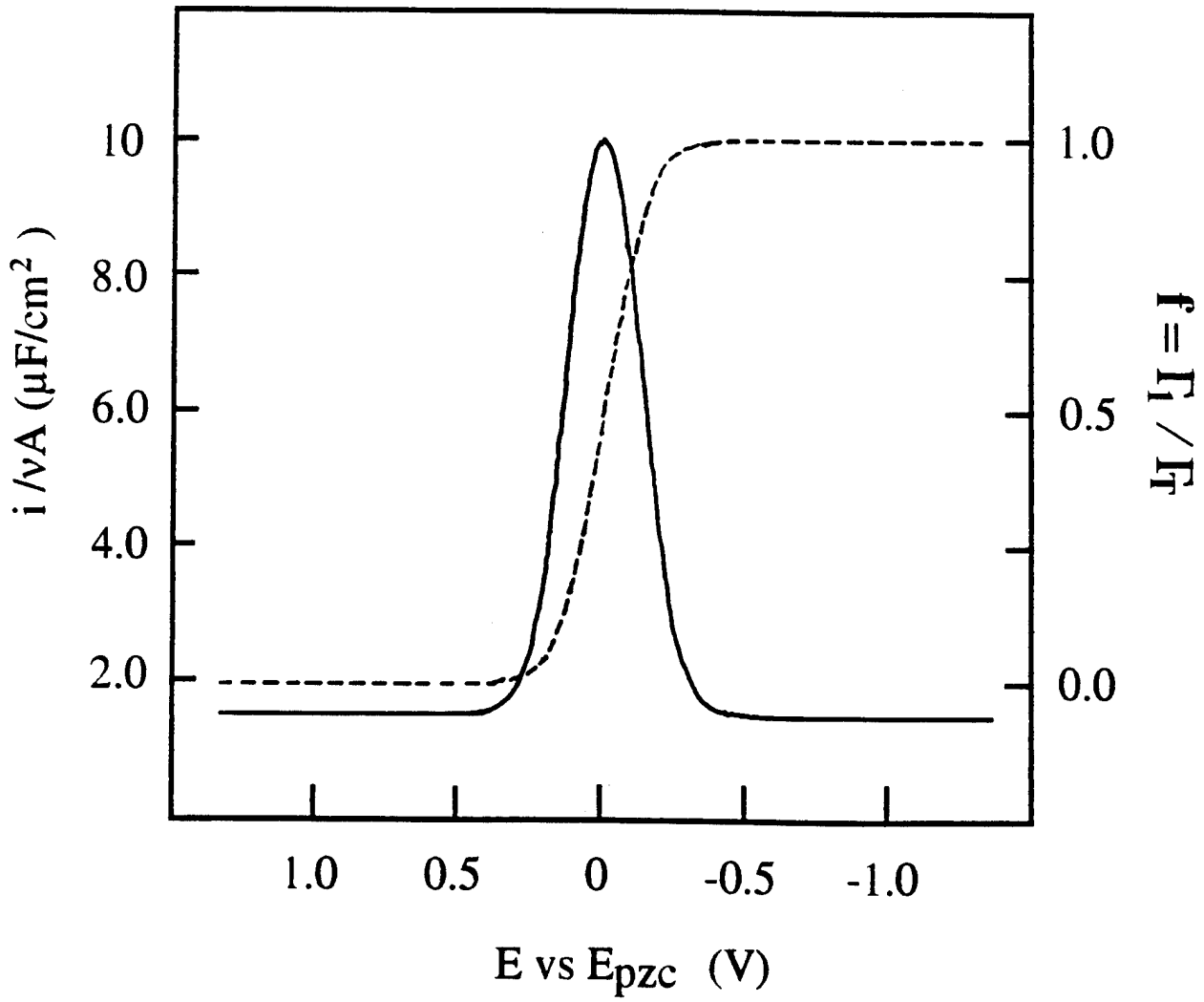

Fig. 4

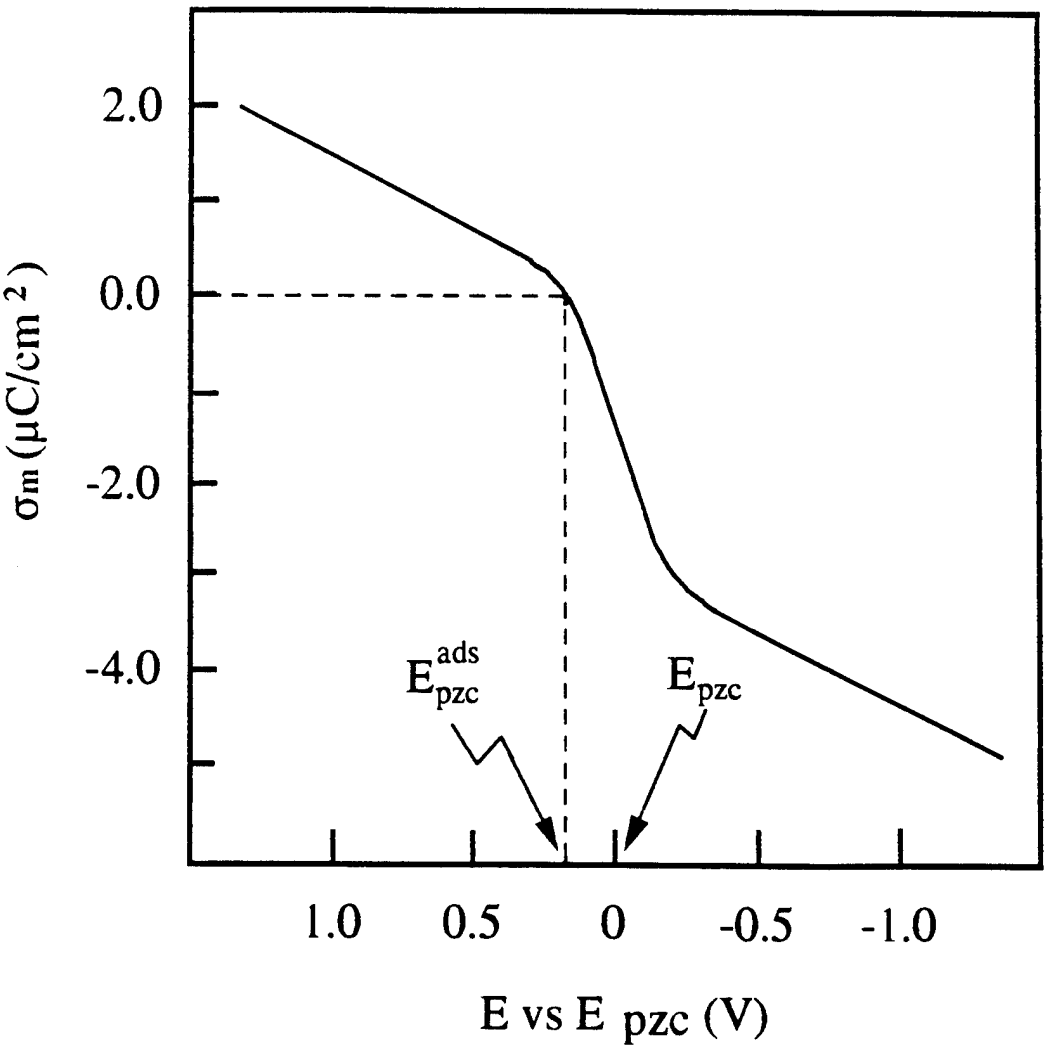

Fig 5

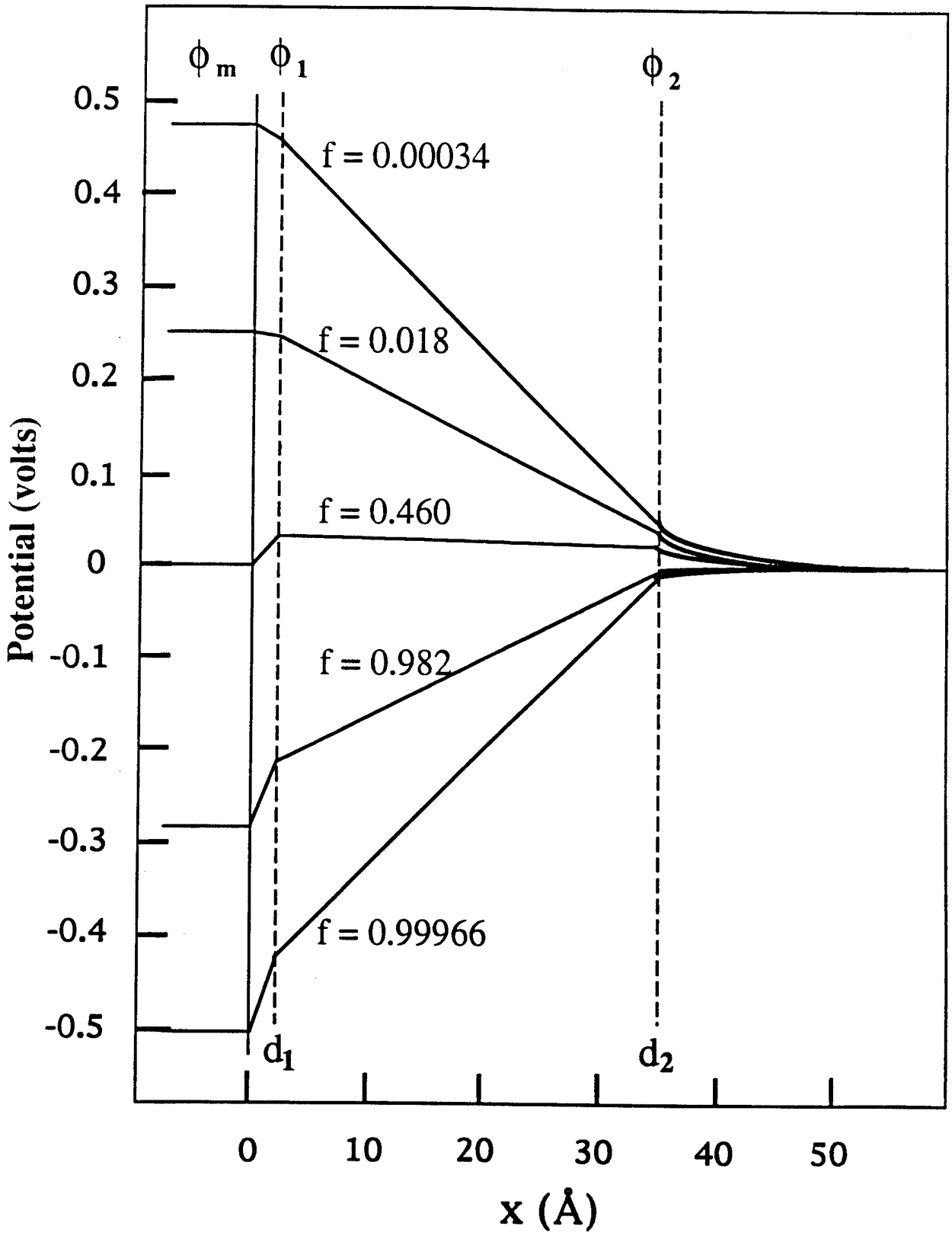
ϕ_m
ϕ_1
ϕ_2
f = 0.00034
f = 0.018
f = 0.460
f = 0.982
f = 0.99966
d_1
d_2
Potential (volts)
0.5
0.4
0.3
0.2
0.1
0
-0.1
-0.2
-0.3
-0.4
-0.5
0
10
20
30
40
50
x (Å)

Fig 6

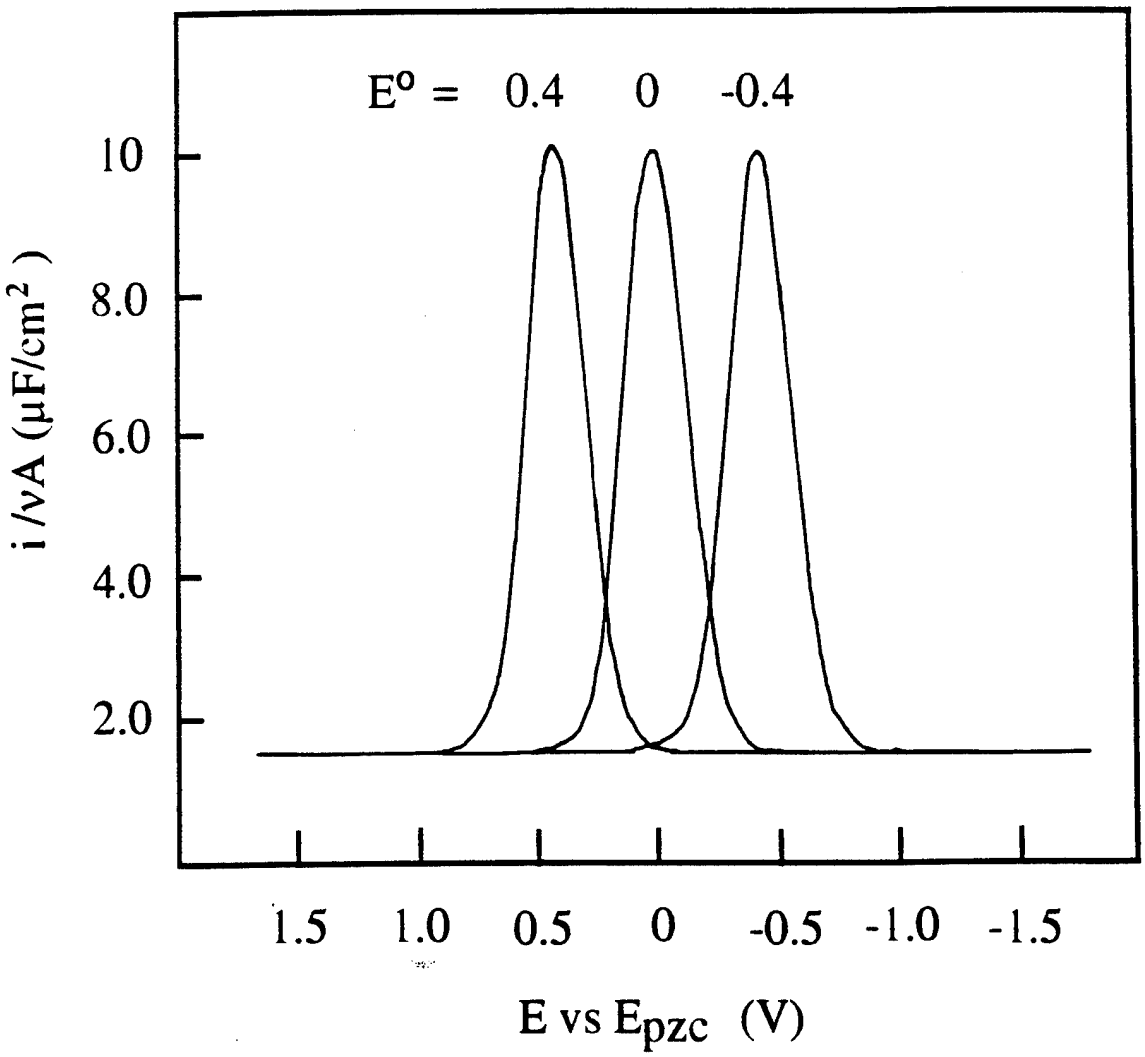

Fig 7

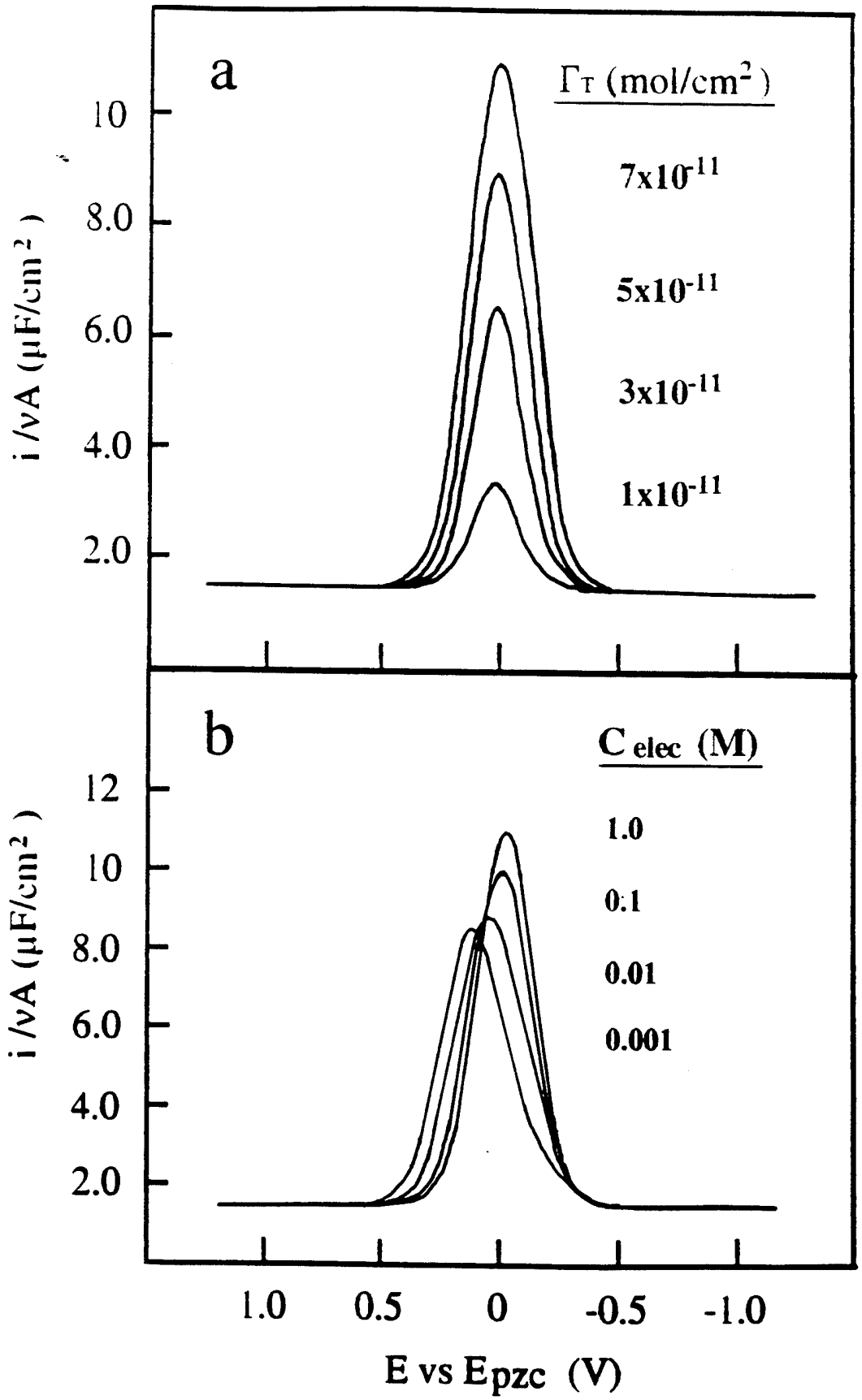
a
Γ_T (mol/cm^2)
7x10^{-11}
5x10^{-11}
3x10^{-11}
1x10^{-11}
i /νA (μF/cm^2)
10
8.0
6.0
4.0
2.0
b
C elec (M)
1.0
0.1
0.01
0.001
i /νA (μF/cm^2)
12
10
8.0
6.0
4.0
2.0
1.0
0.5
0
-0.5
-1.0
E vs Epzc (V)

Fig 8

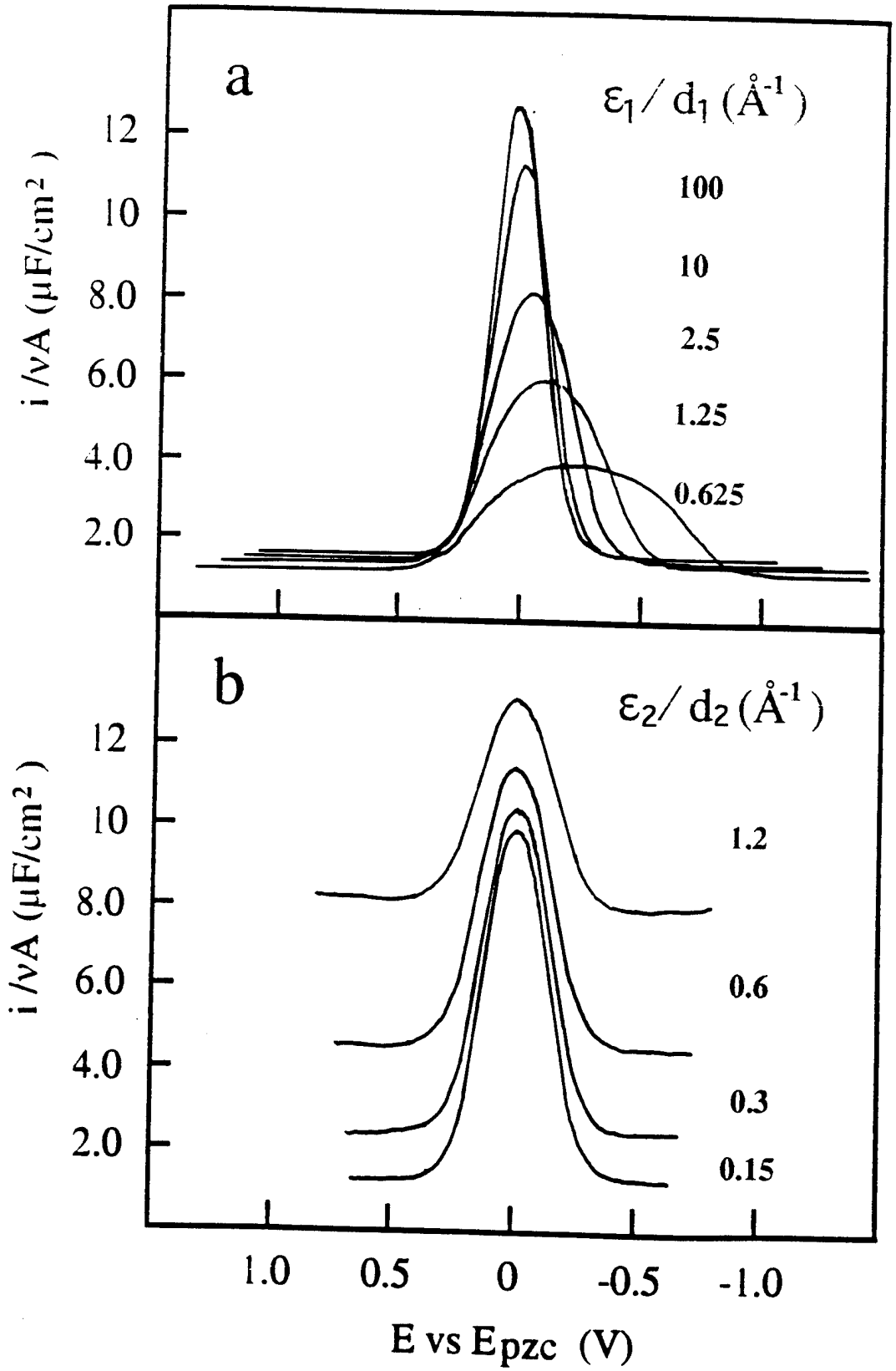
a
ε_1 / d_1 (Å^{-1})
100
10
2.5
1.25
0.625
i /νA (μF/cm^2)
12
10
8.0
6.0
4.0
2.0
b
ε_2 / d_2 (Å^{-1})
1.2
0.6
0.3
0.15
1.0
0.5
0
-0.5
-1.0
E vs Epzc (V)

Fig 9

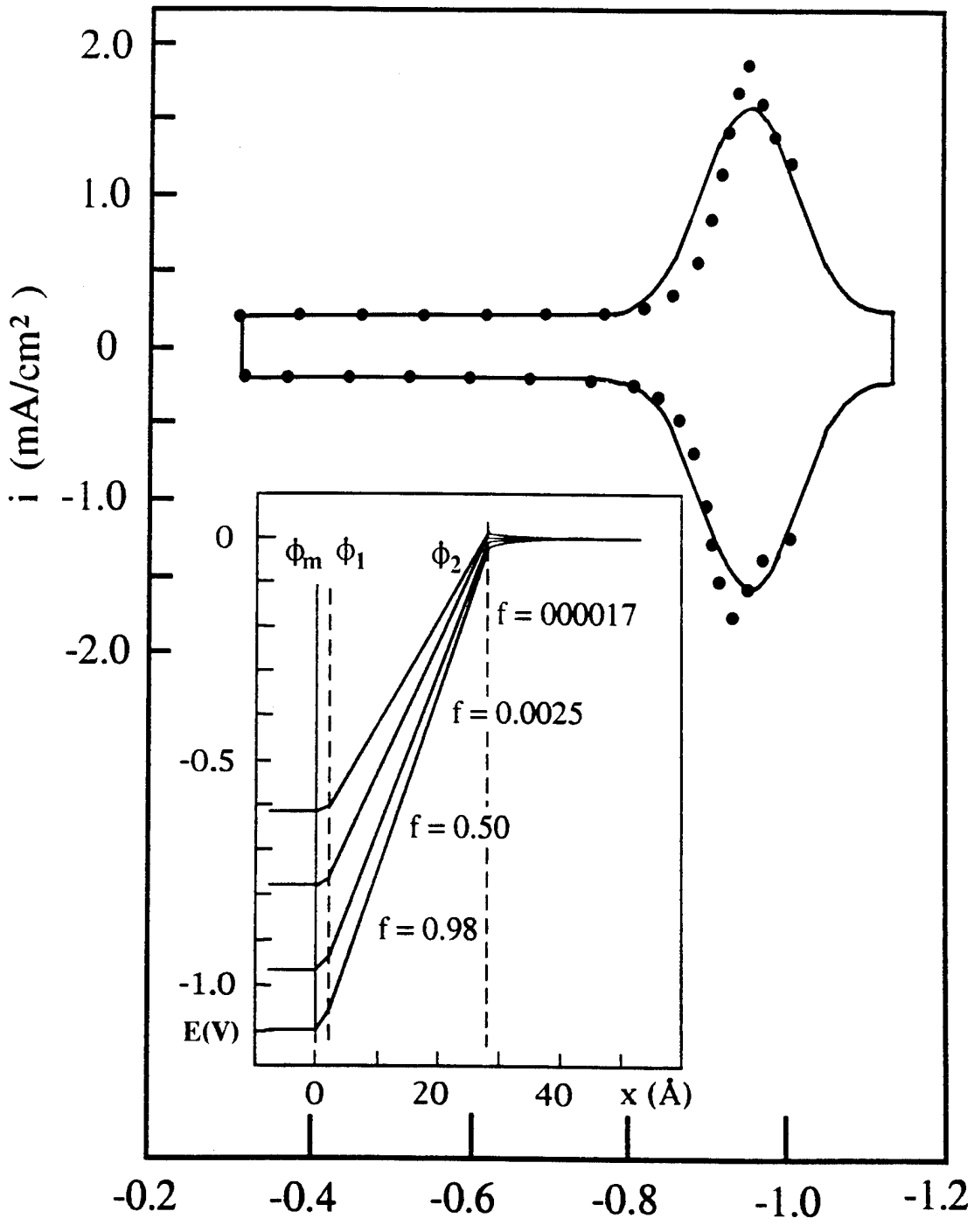
2.0
1.0
0
-1.0
-2.0
i (mA/cm²)
-0.2
-0.4
-0.6
-0.8
-1.0
-1.2
E vs E_SSCE (V)
0
-0.5
-1.0
E(V)
φm φ1
φ2
f = 000017
f = 0.0025
f = 0.50
f = 0.98
0
20
40
x (Å)

Fig 10